

A STUDY OF STRAIN ELASTOGRAPHY UNDER
A NORMAL TENSILE TESTING CONDITION

by

Harish C. Kukatla

Submitted in Partial Fulfillment of the Requirements for

the Degree of

Master of

Computing and Information Systems

YOUNGSTOWN STATE UNIVERSITY

August 2010

A STUDY OF STRAIN ELASTOGRAPHY UNDER
A NORMAL TENSILE TESTING CONDITION

Harish C. Kukatla

I hereby release this thesis to the public. I understand that this thesis will be made available from the OhioLINK ETD Center and the Maag Library Circulation Desk for public access. I also authorize the University or other individuals to make copies of this thesis as needed for scholarly research.

Signature:

Harish C. Kukatla, Student Date

Approvals:

Dr. Yong Zhang, Thesis Advisor Date

Dr. John Sullins, Committee Member Date

Dr. Graciela Perera, Committee Member Date

Peter J. Kasvinsky, Dean of School of Graduate Studies and Research Date

DEDICATION

To my parents, Mr. Subba Rao and Mrs. Vindhya Vali for all their support and belief, also to my brothers, sister – in – law, my niece and nephew.

ABSTRACT

Optical elastography is a new imaging modality that is capable of estimating mechanical properties of a deformed object. However, the current method only provides a relative strain distribution map that may not be adequate for certain medical applications. In this investigation, biomechanical tensile testing is used to calibrate the optical elastogram to estimate the absolute Young's modulus values. This study has two features: (i) Both treated and controlled samples were examined; (ii) Optical flow and strain algorithms were used to compute motion and strain images that characterize tissue property changes during all stages of deformation (linear, plastic and post – rupture). The findings of this study demonstrate that a calibrated optical elastography is a very promising technique to quantify tissue properties *in vivo*.

ACKNOWLEDGEMENTS

I would like to thank Dr. Zhang for giving me the opportunity to work on this research project. Coming from a very different education background than computer science, it would be impossible for me to do a Master Thesis without Dr. Zhang's guidance and encouragement. My sincere thanks also go to Dr. Sullins and Dr. Perera for being the committee members. Finally, I thank my family and friends who gave me the motivation and support that have been invaluable to my life.

TABLE OF CONTENTS

ABSTRACT	IV
ACKNOWLEDGMENTS	V
LIST OF FIGURES	VII
LIST OF TABLES	VIII
1. INTRODUCTION	1
2. RELATED WORKS	2
3. EXPERIMENTS AND METHODS	3
1. SPECIMEN AND BIOMECHANICAL ANALYSIS	3
2. OPTICAL ELASTOGRAPHY	6
4. RESULTS	13
5. DISCUSSION	17
6. CONCLUSIONS	18
7. REFERENCES	19

LIST OF FIGURES

FIGURE 1	5
FIGURE 2	13
FIGURE 3	16
FIGURE 4	17

LIST OF TABLES

TABLE 1	7
TABLE 2	8

1. INTRODUCTION

Optical elastography is a recently developed imaging technology that evaluates the mechanical properties of biological materials using the coherent optical sensors. The majority of elastography studies have focused on cancer detection in internal organs such as prostate, breast and kidney [3, 4, 5]. The elastographic techniques based on ultrasonic sensors need a direct contact of the imaging devices with samples. In this thesis work, a more practical method of calibrating an optical elastogram is described. The method of calibrating an optical elastogram consists of three basic components:

1. Video acquisition using a high definition camcorder that records the tissue deformation process.
2. Video preprocessing using a robust optical flow algorithm.
3. Further processing of optical flow data to obtain strain elastograms that depict the biomechanical property distributions of tissue.

This thesis has two important contributions:

1. As the first calibration study for optical strain elastograms using tensile test results, it establishes a performance baseline for relative strain elastograms.
2. The calibration is carried out with both linear (elastic) and non-linear (plastic) deformations and therefore has strong clinical implications for various skin disease diagnosis and tissue bioengineering.

2. RELATED WORK

An imaging method can be used to capture elasticity distribution on a much finer scale (pixel level). Recently, an optical flow based technique has been developed to compute elasticity and strain images, and has been applied to burn scar assessment [1]. Image-based methods are particularly suited for the soft tissues to which certain mechanical devices cannot be applied. The ideal approach is to integrate elastographic data and point-wise measurements to provide a comprehensive characterization of skin properties [2]. Due to the lack of consensus, more comparative studies are needed in order to establish clinical correlations among different methodologies [6, 7].

One important motivation of this study is that it has been proved that the optical elastography calibrated by the ground truth tests has a strong clinical implication. A calibrated elastogram may provide absolute property values without the need of *in vivo* measurement using excitation force exerted on soft tissue, which is often difficult to collect [9]. This method allows the identification of changes in tissue properties that may not be necessarily visible on skin surface. This type of information is potentially important for clinical repair or surgical intervention [8]. This thesis work is unique in the sense that:

1. The optical elastography is very much similar to the actual elastogram that was derived using the mechanical test instruments.
2. The experiments are conducted for the same tissues with two conditions: treated and controlled. This design allows us to quantitatively analyze the effectiveness of the treatment.

3. EXPERIMENTS AND METHODS

3.1 SPECIMEN AND BIOMECHANICAL ANALYSIS

Specimen Preparation

The rabbit tissue preparation was done at the Departments of Mechanical Engineering and Biology at Youngstown State University. The following paragraphs were taken from the original text of [9], to provide a self-contained description of the experimental procedure.

The specimen preparation involves New Zealand white rabbits and was done in three different stages. The first stage involves harvesting and culturing of MSC's. Stage two involves transplanting MSC's on to rabbit fascia following defect and repair. Finally the third stage involves harvesting fascia following a 8-week surveillance.

The main protocol that involves in harvesting and culturing of MSC's is placing the rabbit under general anesthesia and exposing the proximal medial tibia with a small incision. The medical treatment has given 10-ml syringe with 1 ml of heparin solution. Mononuclear cells were collected from the bone marrow following centrifugation through a Ficoll (1.077g/ml) density gradient (400xg for 30 min at 25°C). After centrifugation, the supernatant was removed and the cells re-suspended in 10ml of Dulbecco's modified Eagle's Medium (DMEM) containing antibiotics, antimycotics and 10% fetal calf serum. The cells were counted with a hemocytometer and 10^6 cells/ml seeded into a T75 culture flask. Once the cells were isolated from the individual rabbits, each of the cell lines were grown separately in labeled flasks.

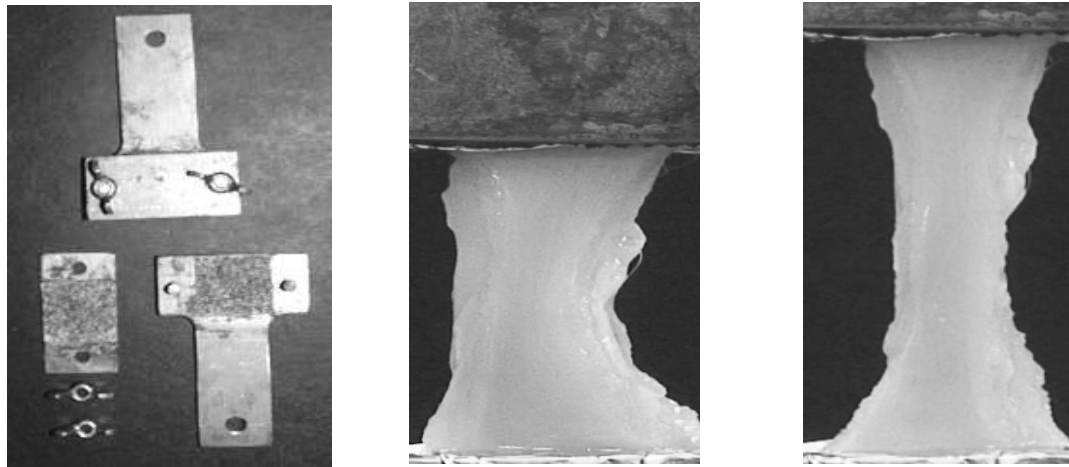
The unattached cells were removed with the existing culture medium and the new complete medium will be added to the flask after four days of primary culture. The same

process will be repeated for every three days till these cells reached eighty percent confluence. Cell passage involved the addition of 3mL aliquot of 0.25% trypsin in 1.0mM EDTA to each flask. Following the addition of trypsin, each plate was incubated for 7 min at 37°C. After the incubation all the cells were transferred to 50mL Falcon tubes and centrifuged at 600xg for 5 minutes followed by re-suspension in DMEM and counted with hemocytometer before passing cells into new T75 culture flasks.

The second stage used a model that allowed the use of each rabbit as its own control. The main part of this method is involved in the creation of a midline abdominal wall skin incision in anesthetized rabbits and is followed by bilateral fascial incisions approximately 6cm in length and 1cm lateral to the midline. The fascial defects were created without entering the peritoneum. The defects following the placement of the materials were closed with 6-0 running nylon sutures. There were two controls, one was located on the right side of the each rabbit and the other one is fixed to observe on the left side of each rabbit. The cell lines were added to the platelet rich plasma enhanced fibrin glue which was removed from culture flasks. Fibrin glue was mixed with isolated MSC's and platelet gel. The PRPFG/Collagen vehicle was placed directly on the facial defect which contains MSC's. By the re-implantation of the cells, the skin was closed with running 4-0 cutaneous sutures and monitored by veterinary staff for a period of 8 weeks. The entire abdominal fascia from all three arms was harvested by the end of the eight weeks of healing and surveillance. The samples with required controlled samples were ready for biomechanical testing.

Biomechanical Testing

The biomechanical properties of tissue samples were determined following the biometrical tensile testing procedure. The tissues were cut into dumbbell shaped pieces across the healed defect using the standard stencils. The specimens were put in saline solution at 37°C in order to keep it disaffected. The tensile testing was performed using an Instron Tensiometer, Model 5500R equipped with a 100N load cell capable of 0.25% accuracy over the entire range. Custom grips were manufactured to reduce the breakage at the attachment sites. Figure 1 shows custom grips that were used and two specimens during the tension test. The tissues were placed between the custom grips using aluminum foil to reduce the contamination. In order to avoid slipping effect, the custom grips had been sand-papered. The wing nuts were finger tightened (Figure 1).



(a) Custom Grips.

(b) Linear Deformation.

(c) Plastic Deformation.

Figure 1: The experiment setup of biomechanical experiments

The tension force was applied at a constant rate to the tissue until the breaking point. Both force and tissue deformation information was recorded to the breaking point. The entire deformation process was videotaped using a Canon XL1s camcorder with a capturing speed of 30 frames per second. The videos were later used for computing flow and strain images.

3.2 OPTICAL ELASTOGRAPHY

Optical elastography uses coherent light techniques to evaluate the mechanical behavior of materials. The focus of this thesis work is to use optical elastography to study the strain distribution of biological tissue under a normal tension testing conditions. Since optical elastography is a noninvasive technique, there will be no direct contact between the samples and the sensor. The variation of the strain tensor can be observed throughout the deformation cycle (linear, plastic and post-rupture). The process of computing the dynamic range of a strain elastogram involves three steps.

1. Capturing tissue deformation and video preprocessing.
2. Computing optical flow.
3. Obtaining a strain elastogram.

Capturing tissue deformation and video preprocessing

Videos were acquired using a Sony HDR-SR1 camcorder with a capture speed of 30 frames per second. Videos were collected in a laboratory under the normal indoor lighting condition. The room temperature was maintained at around 25° C. The distance between the camcorder and the experimental set up was adjusted depending upon the size (width and height) of the specimen. After the camcorder was focused on the whole

experimental set up, the tension was applied to the specimen till it breaks slowly so as to generate the smooth deformation. This process was repeated for every specimen (see Table 1).

Table 1: Specimen Information

Sample	Width (mm)	Length (mm)	Thickness (mm)	Type	Elastogram
14C	12.70	43.89	4.09	Control	No
14T	10.62	52.55	3.56	Treated	Yes
15C	10.69	26.54	3.10	Control	Yes
15T	11.48	31.55	2.87	Treated	No
16C	11.76	26.90	3.66	Control	Yes
16T	11.53	37.80	3.72	Treated	No
17T	11.63	18.72	7.01	Treated	Yes

After being transferred from the camcorder to a computer, videos were split into individual frames using the Sony Vegas Pro-8 editing software. The conversion was done separately for each video. The videos were uploaded to Sony Vegas package followed by picking the start time and the end time of the video sequence. The output image format is JPG. The aspect ratio (the ratio of the width of the image to its height) was set to 1.000 square to ensure that the newly extracted frame has the same size of the original videos. The videos were broken with 30 images per second. All of frame splitting processes were automated using a Perl script.

The JPG files were then converted into PGM files which are in the portable gray map format. A PGM file is an array of integers in the range of 0-255, which makes image processing algorithm easy to implement. Table 2 gives the information of each video sequences analyzed, including the peak time and the peak frame (when the highest point in a stress-strain curve was observed).

Table 2: Video Information with Peak Time and Peak Frame

Date	Video#	Sample Name	Peak Time	Peak Frame	Break Extension	Break Time	Break Frame
4/8/2009	Video4	13C	1:53	3500	53.60	2:30 - 4:00	4500 - 7200
4/8/2009	Video5	14T	2:50	5090	57.47	3:10 - 4:00	5670 - 7200
4/8/2009	Video6	15C	2:20	4280	48.83	3:30 - 4:00	6300 - 7200
4/8/2009	Video7	16C	2:40	4810	60.47	4:30 - 5:30	8000-10000
4/8/2009	Video8	17T	3:05	5500	48.25	3:15 - 3:45	5800 - 6800

Optical Flow Computation

In optical flow computation, an object's deformation was analyzed at the pixel level. A robust optical flow algorithm was used to track the inter-frame motion. Optical flow algorithm is based on the brightness conversation principle as applied to an image. In an optical flow image, the brighter pixels represent larger motions while the darker pixels represent smaller motions. The brightness conservation equation is given below:

$$\frac{\partial I}{\partial x} \frac{dx}{dt} + \frac{\partial I}{\partial y} \frac{dy}{dt} + \frac{\partial I}{\partial t} = 0, \quad (1)$$

In the above equation, I is the image brightness function. x and y as rows and columns of an image and t is the time frame interval between the two frames. The resulting motion vector of a point in an image is given below.

$$u = (u, v)^T, u=dx/dt, v=dy/dt.$$

To find a solution of brightness conservation equation using two adjacent video frames, two fundamental assumptions have to be made:

1. The brightness of a point on a moving object remains constant during the interval of two adjacent frames.
2. The pixels in an image neighborhood (a preset small window or kernel) move with the same or a similar speed. Violation of those two conditions can result in erroneous motion data, which in turn makes the subsequent strain computation inaccurate. To deal with this issue, various robust algorithms have been developed that incorporate both global and local smoothness constraints.

Because of the mathematical ambiguity caused by the aperture problem, Equation (1) doesn't always guarantee a unique and stable solution. The regulation constrains terms have to be imposed for a robust algorithm:

$$obj(u, v) = (I_x u + I_y v + I_t)^2 + \lambda(u_x^2 + u_y^2 + v_x^2 + v_y^2) \quad (2)$$

In the above equation I_x , I_y , u_x , u_y , v_x and v_y denote the partial derivatives of the corresponding variables, and λ is the Lagrange multiplier. The optical flow obtained by minimizing the above objective function is a compromise between the observed motion and the smoothness constraint.

Cumulative Motion across Multiple Frames

So far two adjacent frames were used to compute small motions. Since only two frames were used, it was impossible to examine the large displacements across multiple frames. For this purpose, a large cumulative motion was computed by adding up a series of small motions:

$$u(i, i+n) = u(i, i+1) + u(i+1, i+2) + \dots + u(i+n-1, i+n), \quad (3)$$

$$v(i, i+n) = v(i, i+1) + v(i+1, i+2) + \dots + v(i+n-1, i+n), \quad (4)$$

where $u(i, i+n)$ and $v(i, i+n)$ represent the cumulative motion between Frame i and Frame $i+n$. It is this cumulative motion that is used in the following strain computation. The optimal value of n varies from sequence to sequence. A fixed value of 5 was used in all of the experiments and images of good quality were obtained.

Strain Elastography

The Cauchy strain tensor (ϵ) was adopted to compute strain elastogram from the optical flow results. The Cauchy's equation is given below

$$\epsilon = \begin{bmatrix} \epsilon_{xx} = \frac{\partial u}{\partial x} & \epsilon_{yx} = \frac{1}{2} \left(\frac{\partial u}{\partial y} + \frac{\partial v}{\partial x} \right) \\ \epsilon_{xy} = \frac{1}{2} \left(\frac{\partial v}{\partial x} + \frac{\partial u}{\partial y} \right) & \epsilon_{yy} = \frac{\partial v}{\partial x} \end{bmatrix}, \quad (5)$$

with $(\epsilon_{xx}, \epsilon_{yy})$ as the normal strains and $(\epsilon_{xy}, \epsilon_{yx})$ as the shear strains. Using an optical flow solution $u = (u, v)^T$, the derivatives in (5) can be computed by a convolution operation:

$$\frac{\partial u}{\partial x} = S_x * u, \quad \frac{\partial v}{\partial x} = S_x * v, \quad (6)$$

$$\frac{\partial u}{\partial y} = S_y * u, \quad \frac{\partial v}{\partial y} = S_y * v, \quad (7)$$

where S_x and S_y are the Sobel filters. Given the derivatives, an image is computed for each strain component $(\epsilon_{xx}, \epsilon_{yy}, \epsilon_{xy}, \epsilon_{yx})$. When both horizontal and vertical deformations are significant, a magnitude elastogram can be obtained by:

$$\epsilon_m = \sqrt{\epsilon_{xx}^2 + \epsilon_{xy}^2 + \epsilon_{yx}^2 + \epsilon_{yy}^2} \quad (8)$$

In a tensile test, the motion filed was dominated by the vertical motion. In order to get the most meaningful deformation, emphasis was given to the elastogram of ϵ_{yy} . The strain values were normalized to an intensity range from 0 to 255 for the visualization purpose. The brighter pixel indicates that the strain is higher at the point and the dark pixel explains that there is little or no strain variation. A few sample strain images are given below (Figure 2).

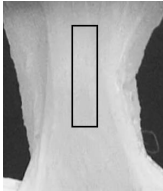
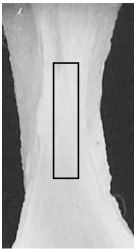
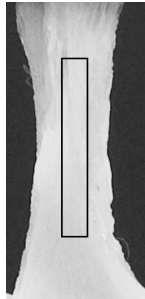

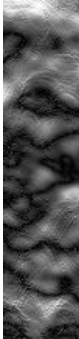

Images of tissue sample and the selected regions for elastogram computation.			
Elastograms			
	Linear Deformation	Plastic Deformation	Post-rupture Deformation

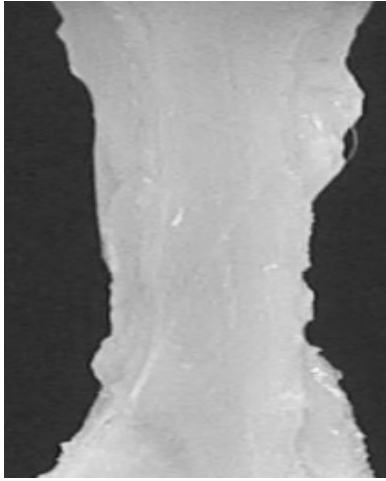
Figure 2: Sample images and corresponding elastograms of 17T at three deformation stages.

4. RESULTS

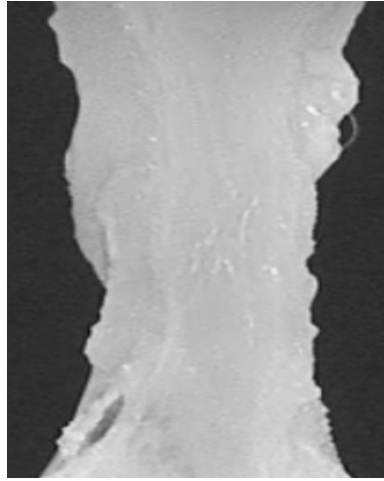
The optical flow and strain elastography results are primarily used to address the following two issues:

1. To describe a tissue sample's biomechanical behavior in three different deformation stages using both flow images and strain elastograms.
2. To identify the factors that could cause flow and strain image artifacts or quality deterioration.

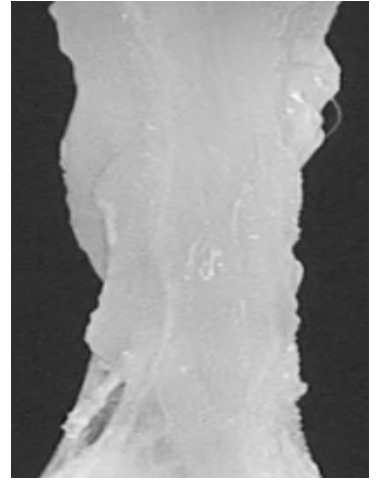
In the first case (Figure 3), image boundaries were set to black pixels, because the background noise sometimes cause sudden changes in the intensity values. Therefore, background pixels were not considered in the computation of optical flow and strain images. Several observations can be made from those images: (i) Both vertical motion and horizontal motion were successfully captured with very good quality that ensures the quality of strain magnitude images; (ii) Although the flow image were normalized, it should be pointed out that vertical motion is much larger than the horizontal motion. In fact, for most samples studied, the difference between horizontal motion and vertical motion could be several orders of magnitude. As a result, the strain values are mainly influenced by the vertical component; (iii) Tissue structure (horizontal layers of muscle fibers) is clearly visible in strain elastograms, which is indicative of the existence of material property heterogeneity; (iv) Due to the lack of enough samples, it is not clear at this point whether the strain patterns observed on elastograms can be correlated to property variations in each deformation stages (linear, plastic and post-rupture) that makes biological and anatomical senses.



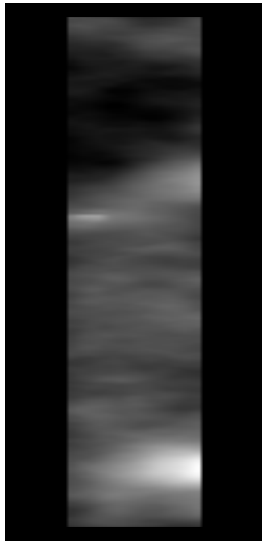
(a) Frame 6508



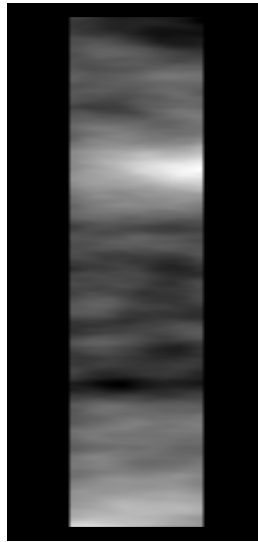
(b) Frame 6719



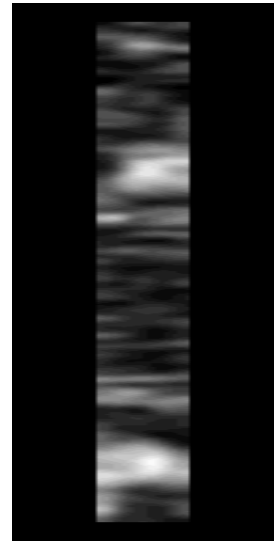
(c) Frame 6939



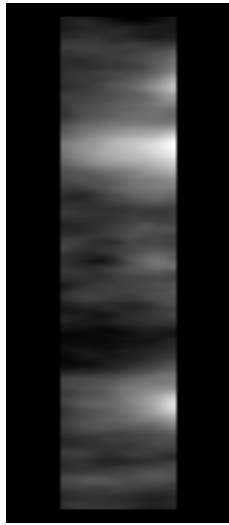
(d) Horizontal Motion



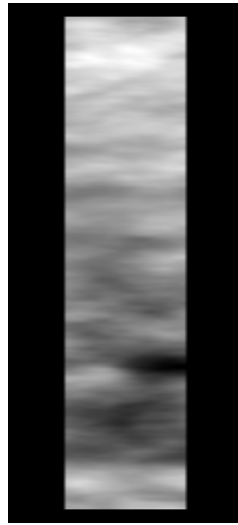
(e) Vertical Motion
Frame 6508 to Frame 6513



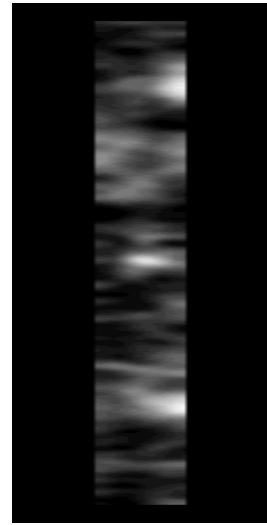
(f) Strain Magnitude



(g) Horizontal Motion



(h) Vertical Motion
Frame 6719 to Frame 6724



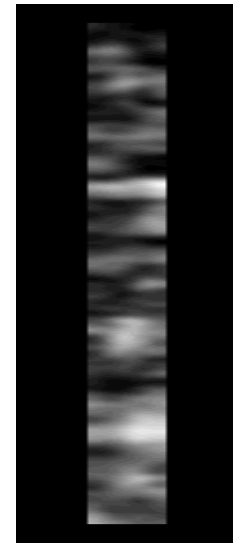
(i) Strain Magnitude



(j) Horizontal Motion



(k) Vertical Motion
Frame 6939 to Frame 6944



(l) Strain Magnitude

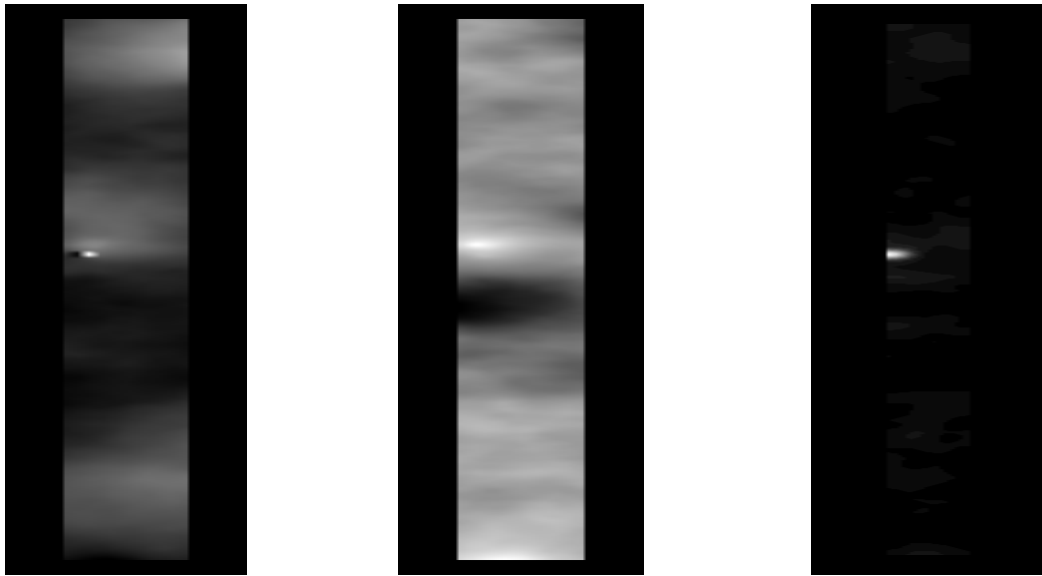
Figure 3: Optical flow and strain images of three video sequences:

(d, e, f) Frame 6508 to Frame 6513.

(g,h, i) Frame 6719 to Frame 6724.

(j, k, l) Frame 6939 to Frame 6944.

In the second case (Figure 4), it was observed that a small background noise could lead to a significant change in optical strain image quality. There was a sudden movement of a piece of tissue in the horizontal direction. This motion is almost negligible in comparison to the vertical motion. However, it generated a very large strain value because strain vector is computed as a first order derivative of the motion field. In other words, strain value is very sensitive to the sudden changes in a motion field, no matter whether it is related to real tissue deformation or caused by lighting condition variations. This type of strain image is often characterized by an isolated spot of very high strain values and should not be used for tissue property analysis, because the interpretation of this type of strain elastogram may result in large errors. A post-processing method that can help provide more quantitative readings is necessary.



(a) Horizontal Motion

(b) Vertical Motion

(c) Strain Magnitude

Figure 4: The flow and strain image for sequence of Frame 6599 to Frame 6604.

5. DISCUSSION

Optical elastography is still in its early development phase. There are many technical issues that need to be addressed before it can be used in a clinical environment. Therefore, a large amount experimental investigation using animal tissues samples is necessary. Based on the results of this research, it was found that relative strain index, optimal number of frames for cumulative motion calculation, and background noise are the key factors that could affect the quality of an elastogram.

Relative Strain Index

Unlike any other current property measuring methods, optical elastography provides a dense pixel-level representation of tissue properties. Although an elastogram does not give absolute Young's modulus with the current imaging sensor because of the lack of Neumann boundary condition constraint, an alternative approach of computing Relative Strain Index (RSI) can be used to quantify tissue properties. RSI is computed by the following formula:

$$RSI = \frac{\frac{1}{m} \sum_{i=1}^m \mathcal{E}_h(i)}{\frac{1}{n} \sum_{j=1}^n \mathcal{E}_d(j)}, \quad (9)$$

where $\mathcal{E}_h(i)$ is the strain value at pixel i of healthy tissue and $\mathcal{E}_d(j)$ is the strain at pixel j of abnormal tissue. m and n are numbers of pixels in two types of tissues.

Optimal Number of Frames for Cumulative Motion Calculation

Optimal number of frames for cumulative motion is also one of the important factors which directly affect the quality of the strain elastogram. The n value should be taken appropriately based on the quality of the video and the tissues physical properties. In this research, a constant value of 5 frames was used for all the video sequences. But, it is not appropriate to keep the same n value for other experiments. Its value should be changed according to the quality of the video and a particular testing condition.

6. CONCLUSION

A preliminary experimental study was conducted that examines the biomechanical property variations of rabbit tissues under a large deformation using both elastographic method and tensile testing method. It was found that a strain elastogram computed from optical flow data can yield much detailed information about the spatial distribution of elastic parameters that otherwise would be impossible with the conventional mechanical measuring devices. On the other hands, a tensile test provides absolute Young's modulus value that is lack in a relatively strain elastogram. In future investigation, an optical elastogram should be calibrated by both mechanical testing and finite element modeling to provide a more comprehensive description of tissue property in both laboratory and clinical settings.

7. REFERENCES

- [1] Zhang Y, Goldgof DB, Sarkar S, Tsap LV. A modeling approach for burn scar assessment using natural features and elastic property. *IEEE Transactions on Medical Imaging*, 2004; 10:1325-1329.
- [2] Zhang Y, Sullins JR, Goldgof DB, Manohar V. Computing strain elastogram's of skin using an optical flow based method. *Proceed. of 5th Inter. Conf. on Ultrasonic Measurement and Imaging of Tissue Elasticity*, Snowbird, Utah, October, 2006.
- [3] Souchon R, Rouviere O, Gelet A, Detti V, Srinivasan S, Ophir J, Chapelon JY. Visualization of HIFU lesions using elastography of the human prostate in vivo: preliminary results. *Ultrasound in Medicine and Biology*, 2003; 29:1007-1015.
- [4] Plewes DB, Bishop J, Samani A, Sciarretta J. Visualization and quantification of breast cancer biomechanical properties with magnetic resonance elastography. *Physics in Medicine and Biology*, 2000; 45:1591-1610.
- [5] Kallel F, Ophir J, Magee K, Krouskop TA. Elastographic imaging of low-contrast elastic modulus distributions in tissue. *Ultrasound in Medicine and Biology*, 1998; 24:409-425.
- [6] Jemec GBE, Selvaag E, Agren M, Wulf HC. Measurement of the mechanical properties of skin with ballistometer and suction cup. *Skin Research and Technology*, 2001; 7: 122-126.
- [7] Pedersen L, Hansen B, Jemec GBE. Mechanical properties of the skin: A comparison between two suction cup methods. *Skin Research and Technology*, 2003; 9: 111-115.

- [8] Zhang Y., Brodell R. T., Mostow E. N., Vinyard C. J., and Marie H., In vivo skin elastography with high definition optical videos. *Skin Research and Technology*, 2009; 15: 271-282.
- [9] Marie H., Zhang Y., Heffner J., Dorion A. H., and Fagan L. D., Biomechanical and Elastographic Analysis of Wound Healing Effect using Mesenchymal Stromal Cell Treated Tissue following Surgery, *Journal of Biomechanical Engineering* (in press).

Northeastern Ohio Universities College of Medicine

TO: Jeremy J. Heffner, M.D. – Surgical Education
St. Elizabeth Health Center

FROM: Donna King, Ph.D.
Chairperson, Institutional Animal Care and Use Committee

SUBJECT: Protocol Approval by the Northeastern Ohio Universities College of Medicine
(NEOUCOM) Institutional Animal Care and Use Committee (IACUC)

DATE: May 29, 2007

The following NEOUCOM protocol was reviewed and approved by this Institution's Animal Care and Use Committee (IACUC) on May 29, 2007. This protocol is approved for a three (3) year period of time; however you must submit an annual renewal to the IACUC each year for review. Protocols involving the use of human tissues require Institutional Review Board (IRB) approval. Any serious or adverse events regarding the use of animals approved in this study must be reported immediately to the IACUC Chairperson or the Attending Veterinarian.

NEOUCOM Protocol No.:	#07-012
Title of Protocol:	Autologous Mesenchymal Stem cell Transplantation to Improve Fascial Repair
Type of Vertebrate:	Rabbits
Funding Agency:	St. Elizabeth Surgery Education and Research Fund
Protocol Expiration Date:	May 29, 2010

This institution has an Animal Welfare Assurance on file with the Office of Laboratory Animal Welfare (OLAW). The Assurance number is A3474-01. This institution is also registered with the United States Department of Agriculture (USDA). The USDA registration number is 31-R-0092.

The Comparative Medicine Unit (CMU) at the Northeastern Ohio Universities College of Medicine (NEOUCOM) has been accredited with the Association for Assessment for Accreditation of Laboratory Animal Care (AAALAC) International since June 8, 1982. Full accreditation was last renewed on June 29, 2005.

Thank you.

DK:lkn

Cc: Walter E. Horton, Jr., Ph.D.
Vice President for Research
NEOUCOM Institutional Official

File